Mass Transfer in Rectangular Cavities

E. L. JARRETT and T. L. SWEENEY

Ohio State University, Columbus, Ohio

The captured vortex system produced by the flow of a fluid along a plate containing a transverse rectangular cavity was investigated by measuring the local mass transfer coefficient k_g on the cavity walls. Both transverse and peripheral k_g profiles are presented for cavity depth-to-length ratios of 0.5, 1.0, and 2.0 at free-stream velocities of 6.8, 13.5, and 27 ft./sec. for water evaporating into air. These profiles reflect the three-dimensional nature of the flow in the cavity.

When fluid flows along a plate in which a transverse rectangular cavity is present, a flow system, which is characterized by captured vortices, becomes established in the cavity. The vortex system in the cavity is separated from the free stream by a detached shear layer, as indicated in Figure 1. The behavior of fluid in the cavity, the residence time of material in the cavity, and the transfer coefficients on the internal walls of the cavity are of interest in attempts to model certain heat and mass transfer equipment. There are also aerodynamic applications relative to both subsonic and supersonic flows.

Transport processes at the cavity walls are influenced by the character of the vortex system in the cavity, which is determined by the geometry of the rectangular cavity and its interaction with the flowing fluid in some unexplained manner. This work presents local mass transfer coefficients over the inside of a rectangular cavity and an interpretation of the flow field in the cavity based upon variation in the local mass transfer coefficient and upon visual observation. The local mass transfer coefficients were obtained in a manner which would detect three-dimensional effects. There is not unanimous agreement in the recent literature concerning the existence of these effects.

In the following discussion, for a rectangular cavity as indicated in Figure 2, *transverse* will refer to the horizontal direction normal to the upstream air flow, *longitudinal* will refer to the horizontal direction parallel to upstream air flow, and *vertical* will refer to the vertical direction of Figure 2. *Peripheral* will refer to a path beginning at the top edge of the front wall and continuing vertically down the front wall, longitudinally across the floor, and then vertically up the back wall to the top edge of the back wall.

Roshko (*10*) has investigated pressure distribution on the walls and floor of a rectangular cavity at free stream velocities from 75 to 210 ft./sec. The pressure coefficient profiles around the periphery for cavities of depth D to length L ratios from 0.75 to 2.50 support the theory of one or more large vortices rotating in the cavity, complemented by small vortices at the bottom corners.

Charwat et al. (*2, 3*) postulated pulsations of the detached shear layer in and out of the cavity to account for the strong interchange of mass between the cavity and the external flow. Maull and East (*8*) used oil film patterns and pressure measurements to demonstrate that the flow in the cavity was highly three-dimensional in certain rectangular cavity shapes. The cellular pattern which was observed was regular, and transverse components of velocity along the cavity floor were noted in the streamlines within a cell. Seban and Fox (*12*) measured velocities and heat transfer coefficients in cavities for D/L of 0.29 and 0.54 at 190 ft./sec. free-stream velocity.

Fox has recently investigated flow regimes (*4, 5*) and heat transfer (*6*) in rectangular cavities with D/L of 0.57 to 4.0 at air velocities from 160 to 600 ft./sec. He observed no regular pattern in the dust which had accumulated in his equipment during operation and concluded that the flow was substantially two dimensional. Recently, Seban (*11*) has reported heat transfer and flow characteristics for shallow cavities (D/L of 0.2 to 0.5) and has noted the existence of three-dimensional effects on the front wall.

Burrgraf (*1*) and Mills (*9*) have investigated two-dimensional mathematical models for steady separated flow in rectangular cavities in terms of streamlines, velocities, and other flow characteristics.

EXPERIMENTAL WORK

The device which was used for the measurement of local mass flux is illustrated in Figure 3. A precision bore capillary tube of ⅛-in. I.D. was mounted in the plastic wall of the cavity. The end of the tube in the wall was plugged with a small roll of blotting paper which was shredded at the outer end to make intimate contact with a ¼-in. diameter disk of blotting paper. The outer side of this blotting paper disk, constituting the evaporative surface, was mounted flush with the cavity surface.

Water was introduced into the open end of the tube, and capillary action in the blotting paper kept the surface wet. At the mass transfer rates experienced, the surface was observed to be uniformly wet when the surface pointed either upward or horizontally. The rate of evaporation of water was estimated by measuring the rate of decrease of the length of water in the capillary tube.

The rectangular cavity was installed in the bottom of a rectangular duct, 2 ft. by 6 in. in cross section and 12 ft. long, near the downstream end of the duct. Air was supplied to the rectangular duct by a 6-in. diameter duct from a building supply blower located over 100 ft. away. The transverse dimension (span) of the cavity was 2 ft. and the longitudinal

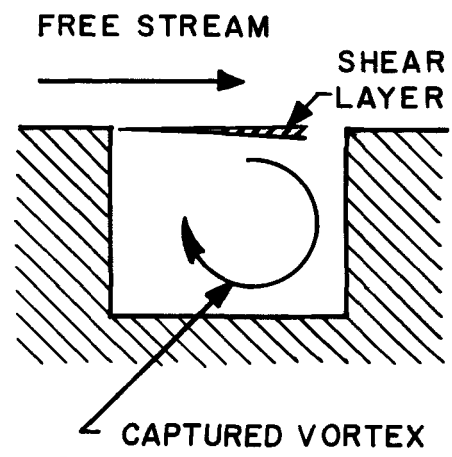

Fig. 1. Flow across a rectangular cavity.

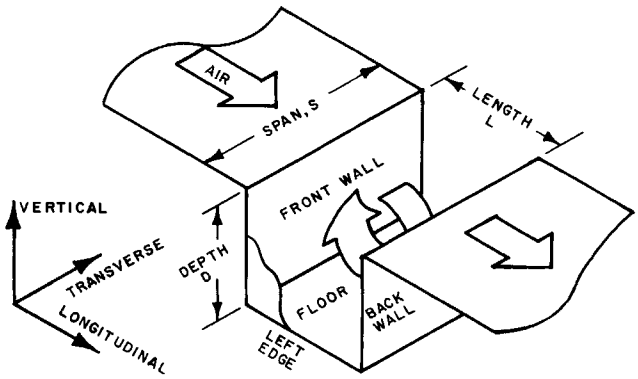

Fig. 2. Rectangular cavity.

dimension (length) was 4 in. The depth of the cavity was continuously adjustable from 0 to 8 in. The walls and floor of the cavity were constructed of ½-in. transparent acrylic plastic sheet.

An array of 147 capillary tubes with blotting paper evaporative surfaces was installed in the walls and floor of the cavity to provide peripheral and transverse flux profiles. Scales were attached to the tubes to facilitate reading of the lengths of liquid in the tubes to within 0.3 mm. During a run the length of liquid in each tube was observed visually four or five times at intervals of 20 min. to 1 hr.

The velocity of the free stream, as measured by a Pitot-static tube, and the wet and dry bulb temperatures of the air were reasonably constant during each run. Cavities with depth to length ratios (D/L) of 0.0, 0.5, 1.0, and 2.0 were investigated at air velocities of 6.8, 13.5, and 27 ft./sec., corresponding to Reynolds numbers in the duct of 50,000, 100,000, and 200,000 based on the hydraulic diameter d_e of the duct (1.33 ft.). Since the length-to-hydraulic diameter ratio for the rectangular duct upstream of the cavity was about 10, the flow was not fully developed. Limited visual observations of the flow in the cavity were made by using a streamer on a probe.

The rate of decrease of the length of liquid in each capillary tube was determined by fitting a least-squares straight line to the plot of length λ vs. time θ. Noting that the area for evaporation was four times the cross-sectional area of the tube, we calculated the molar flux of the evaporating water by

$$\phi = -\left(\frac{\rho_{liq}}{4\,M_{liq}}\right)\left(\frac{d\lambda}{d\theta}\right) \qquad (1)$$

Dividing the molar flux by the driving force based on partial pressure $P_{AO} - P_A$ (where P_{AO} was the water vapor pressure at the evaporation temperature and P_A was the free-stream water partial pressure), we obtained the mass transfer coefficient:

$$k_g = \frac{-\rho_{liq}}{4\,M_{liq}\,(P_{AO} - P_A)}\left(\frac{d\lambda}{d\theta}\right) \qquad (2)$$

From thermocouple measurements of the evaporative surface temperature, a correlation was developed that related the difference between the evaporative surface temperature and the dry-bulb temperature to the molar flux. This correlation was used to calculate the evaporative surface temperature for each datum point.

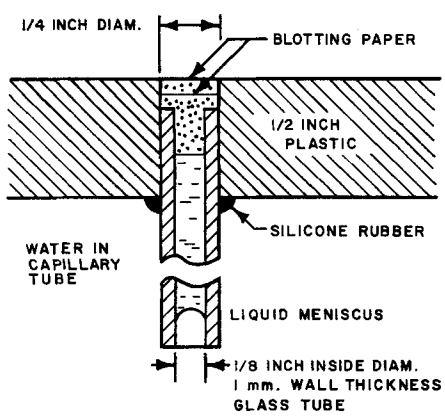

Fig. 3. Device used for mass flux measurement.

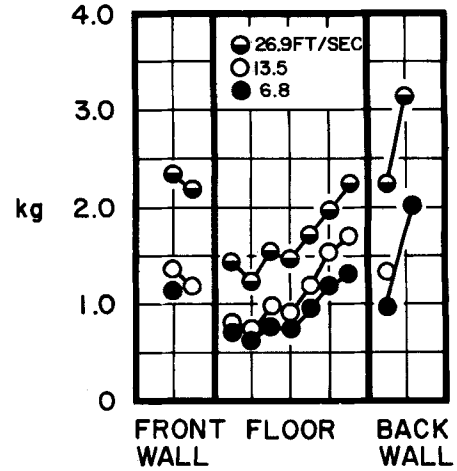

Fig. 4. Peripheral mass transfer profile in the rectangular cavity, k_g [lb.-moles/(hr.)(sq.ft.)(atm.)], D = 2.0 in., L = 4.0 in., parameter is U_∞.

PERIPHERAL MASS TRANSFER PROFILES

The peripheral variation in mass transfer was determined at the center line and at 6 and 11.5 in. on either side of the center line for the three cavity depths and three air velocities investigated. The peripheral variations along the center line are shown in Figures 4, 5, and 6; peripheral variations along the other four lines of observation parallel those of the center line. Note that the variations are large, exceeding any which might be attributed to experimental error.

Equating heat and mass transfer j factors, we calculated peripheral mass transfer coefficient profiles from the peripheral heat transfer coefficient profiles reported by Fox (6). The coefficients were extrapolated from the lowest velocity of Fox (160 ft./sec.) to the highest velocity of this work (27 ft./sec.) by using the 0.8 exponent for the free-stream velocity employed by Fox in his correlation. Substantial agreement in general shape was obtained between the profiles calculated from the work of Fox and those reported here, although the coefficients calculated from Fox's data were only 50 to 70% as large as those reported here.

Two-dimensional vortex systems have been postulated and observed which will satisfy many features of the

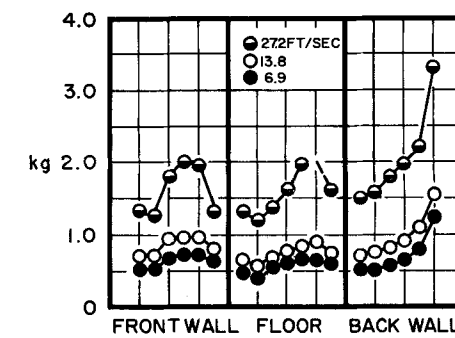

Fig. 5. Peripheral mass transfer profile in the rectangular cavity, k_g [lb.-moles/(hr.)(sq.ft.)(atm.)], D = 4.0 in., L = 4.0 in., parameter is U_∞.

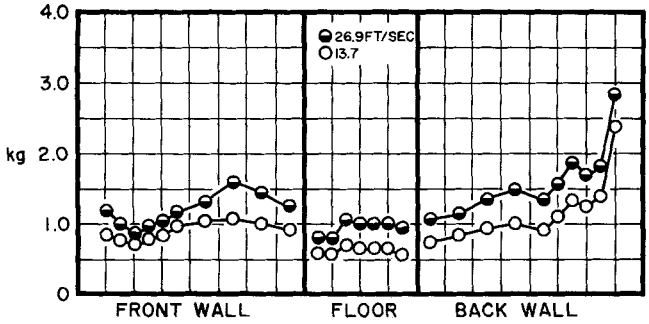

Fig. 6. Peripheral mass transfer profile in the rectangular cavity, k_g [lb.-moles/(hr.)(sq.ft.)(atm.)], D = 8.0 in., L = 4.0 in., parameter is U_∞

peripheral mass transfer coefficient profiles. The highest value of the mass transfer coefficient occurs where the separated free shear layer strikes the top of the back wall of the cavity. This value is similar for the three cavity depths studied.

In the 2-in. by 4-in. cavity, that is, $D/L = 0.5$, the three humps in the floor profile reflect the three vortices in the cavity—two main vortices rotating in the same direction to give a backflow along the floor and a small countervortex in the front corner, as indicated in Figure 7.

In the 4-in. by 4-in. cavity, that is, $D/L = 1.0$, the data may be resolved by considering one large captured vortex, giving a backflow along the floor, and two small vortices in the corners rotating counter to the main vortex. This is sketched in Figure 8.

Similarly, in the 8-in. by 4-in. cavity, where $D/L = 2.0$, one large captured vortex was observed, although two smaller vortices actually may have been present. The relatively low velocity precluded accurate visualization with a streamer. In addition to the principal vortex or vortices, two small corner vortices are also postulated for this ratio of dimensions, as indicated in Figure 9.

TRANSVERSE MASS TRANSFER PROFILES

Important also are the variations in mass transfer along the span of the rectangular cavity. Transverse lines of observation were located at 1.5 and 2.5 in. from the top along the front and back walls and at 1.5 and 2.5 in. from the front wall on the 4-in. floor of the cavity. Typical plots of the transverse variation in mass transfer coefficient k_g along a line of observation are presented in Figures 10, 11, and 12 for the three velocities and three cavity depths studied. The remainder of the transverse profiles are contained in reference 7. The transverse profiles reflect the regular three-dimensional effects in the cavity and in most cases have about four distinct humps of comparable size. Maull and East (8) have reported similar variations in the pressure coefficient and visual observation of these "cells" by oil film patterns.

In the 8-in. by 4-in. cavity ($D/L = 2.0$) at a velocity of 27 ft./sec., the nodal points or mass-flux minima along the floor were nearly evenly spaced along the span. A streamer placed near the floor between two nodes showed rapid fluctuation from side to side, in addition to indicating the general backflow along the floor. This fluctuation is attributed to a shifting between two three-dimensional vortex flow patterns, perhaps associated with the exchange of material between cavity and free stream. It was found that the flow patterns could be stabilized by bleeding a small amount of air from the bottom of the cavity at either the right or left edge of the floor. Under conditions of air bleeding, temporal fluctuations in sign of the transverse component of velocity along the cavity floor ceased. The sign of this velocity component did change with position, however, indicating the presence of four three-dimensional cells. The observations agree with the streamlines within a cell described by Maull and East (8).

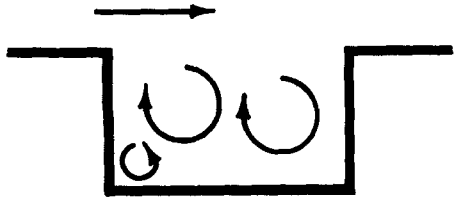

Fig. 7. Approximate streamlines in the rectangular cavity with $D/L = 0.5$.

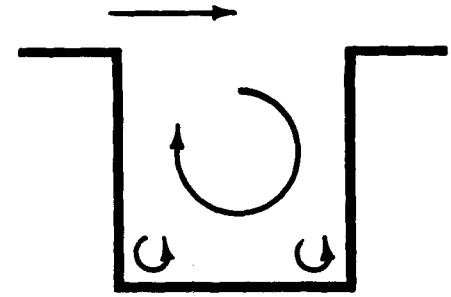

Fig. 8. Approximate streamlines in the rectangular cavity with $D/L = 2.0$.

It is postulated that these cells represent parallel vortex rings whose overall rotation about a transverse axis constitutes the principal vortex, the peripheral effects of which are discussed above. Within each ring the sign of vorticity about a somewhat circular axis of vorticity fluctuates rapidly unless one configuration is stabilized. The zero transverse component of velocity in the plane where two parallel vortex rings touch would yield lower resultant velocity and lower mass transfer rates where this plane intersects the walls and floor of the cavity.

RELIABILITY OF DATA

The slopes of the liquid length vs. time curves were found to be constant for each tube at a given set of conditions, independent of the length of water in the tube. Statistical analysis of the least-squares fit generally indicated confidence limits for the slope of less than 10%,

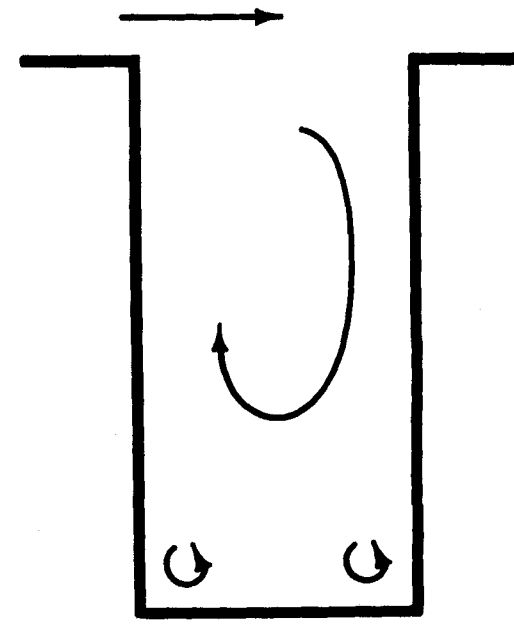

Fig. 9. Approximate streamlines in the rectangular cavity with $D/L = 2.0$

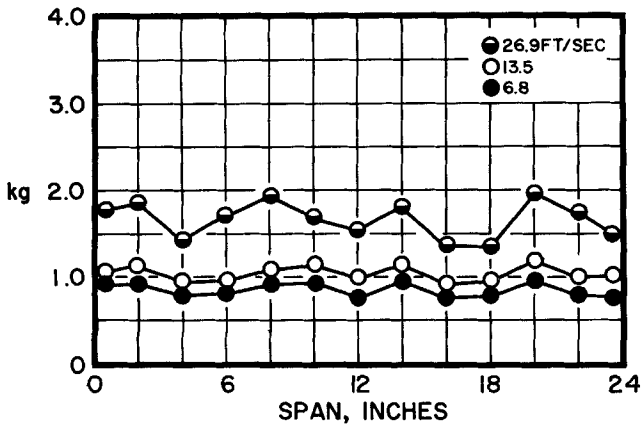

Fig. 10. Transverse mass transfer profile on the floor of the rectangular cavity, 1.5 in. from the front wall, k_g [lb.-moles/(hr.)(sq.ft.)(atm.)], D = 2.0 in., L = 4.0 in., parameter is U_∞

based on a 95% confidence level.

Limitations on the accuracy and precision of the mass transfer coefficients reported herein arise principally from four sources: the assumption that the evaporative surface is flush with the wall; the possibility of surface irregularities; the estimation of the evaporative surface temperature; and the estimation of the slope of the liquid length vs. time line.

CONCLUDING REMARKS

The results derived from the present work may be summarized as follows:

1. A mass transfer technique involving a blotting paper evaporative surface wetted by a capillary tube has provided good results at the low fluxes encountered.
2. Local mass transfer coefficients have been reported which substantially define the mass transfer variation on the walls and floor of the rectangular cavity in both the transverse and peripheral directions.
3. The three-dimensional behavior of the cavity has been conclusively established for the several sets of conditions considered.
4. A system of vortices and vortex rings has been hypothesized to account for the transverse and peripheral variations in mass transfer which were observed.

ACKNOWLEDGMENT

Fellowships granted by The Ohio State University and the National Science Foundation are gratefully acknowledged. Computations were performed at the Numerical Computation Laboratory of The Ohio State University.

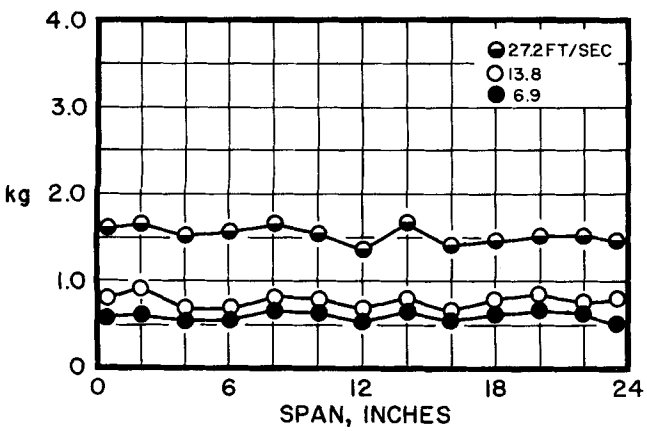

Fig. 11. Transverse mass transfer profile on the floor of the rectangular cavity, 1.5 in. from the front wall, k_g [lb.-moles/(hr.)(sq.ft.)(atm.)], D = 4.0 in., L = 4.0 in., parameter is U_∞.

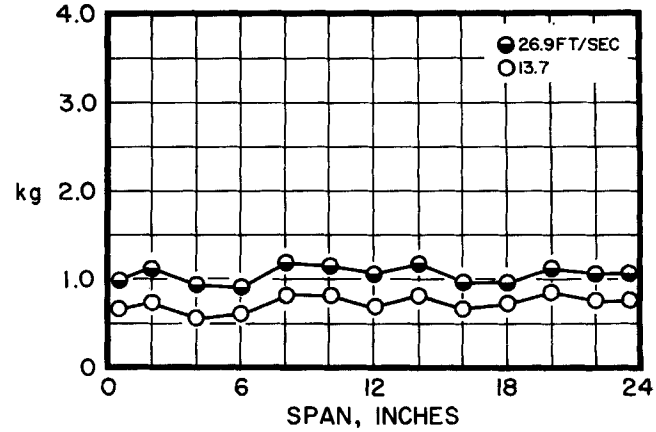

Fig. 12. Transverse mass transfer profile on the floor of the rectangular cavity, 1.5 in. from the front wall, k_g [lb.-moles/(hr.)(sq.ft.)(atm.)], D = 8.0 in., L = 4.0 in., parameter is U_∞.

NOTATION

d_e = hydraulic diameter = 4 (area for flow)/(wetted perimeter), ft.
D = depth of the cavity as defined in the text, in.
k_g = mass transfer coefficient, lb.-mole/(sq.ft.)(hr.)(atm.)
L = length of the cavity as defined in the text, in.
M_{liq} = molecular weight of the liquid evaporating
P_A = bulk partial pressure of water in the air supply, atm.
P_{AO} = saturation vapor pressure of the liquid at the temperature of evaporation, atm.
S = span of the cavity as defined in the text, in.
U_∞ = average velocity in the rectangular duct

Greek Letters

λ = length of liquid in a capillary tube
ρ_{liq} = density of the evaporating liquid, lb./cu.ft.
θ = time, hr.
ϕ = molar flux of evaporating liquid, lb.-mole/(sq.ft.)(hr.)

LITERATURE CITED

1. Burrgraf, O. R., in "Proc. 1965 Heat Transfer and Fluid Mechanics Institute," A. F. Charwat, ed., p. 190, Stanford Univ. Press, Calif. (1965).
2. Charwat, A. F., C. F. Dewey, J. N. Roos, and J. A. Hitz, *J. Aerospace Sci.*, **28**, 457 (1961).
3. *Ibid.*, 513 (1961).
4. Fox, J., in "Proc. 1965 Heat Transfer and Fluid Mechanics Institute," A. F. Charwat, ed., p. 230, Stanford Univ. Press, Calif. (1965).
5. ———, *Natl. Aeronaut. Space Admin. Note D-2501* (1964).
6. ———, *Intern. J. Heat Mass Transfer*, **8**, 269 (1965).
7. Jarrett, E. L., M.Sc. thesis, Ohio State Univ. Columbus (1966).
8. Maull, D. J., and L. F. East, *J. Fluid Mech.*, **16**, Pt. 4, 620 (1963).
9. Mills, R. D., *J. Royal Aeronaut. Soc.*, **69**, 714 (1965).
10. Roshko, A., *Natl. Advisory Comm. Aeronaut. Tech. Note 3488* (1955).
11. Seban, R. A., *Intern. J. Heat Mass Transfer*, **8**, 1353 (1965).
12. ———, and J. Fox, "International Developments in Heat Transfer: Proc. 1961-62 Heat Transfer Conf.," p. 426, Am. Soc. Mech. Engrs., New York (1963).

Manuscript received December 30, 1965; revision received November 11, 1966; paper accepted November 12, 1966.